Journal of the American College of Cardiology Vol. 52, No. 14, 2008

Published by Elsevier Inc.
ISSN 0735-1097/08/$34.00
doi:10.1016/j.jacc.2008.05.059

Prevalence of Different Gadolinium Enhancement Patterns in Patients After Heart Transplantation

Henning Steen, MD, Constanze Merten, MD, Sonja Refle, MD, Roland Klingenberg, MD, Thomas Dengler, MD, Evangelos Giannitsis, MD, Hugo A. Katus, MD

Heidelberg, Germany

Objectives Transplant coronary artery disease (TCAD) limits long-term survival after heart transplantation (HTX). We hypothesized that contrast-enhanced magnetic resonance imaging (CE-MRI) detects chronic TCAD-related myocardial infarctions (MIs), even in patients with angiographically classified mild TCAD.

Background Coronary angiography underestimates the TCAD-degree, subsequently missing occluded small coronary arteries and resulting MI. CE-MRI as a noninvasive imaging technique identifies infarct-typical MI and myocardial fibrosis.

Methods CE-MRI (gadolinium: 0.2 mmol/kg/bw) was performed in 53 HTX patients on a 1.5-T MRI scanner (Philips, Best, the Netherlands). Infarct-typical CE-MRI areas were classified as: I = ≤25%, II = 25% to 50%, III = 50% to 75% and IV = ≥75%. Infarct-atypical forms were divided into diffuse, spotted, intramural, and infero-septal. Coronary angiography results were reviewed qualitatively with the TCAD score (TCAD I = mild evidence; II = 30% to 75%, III = ≥75% stenosis). Groups were compared with analysis of variance (statistically significant p values ≤0.05).

Results Infarct-typical CE-MRI was already present in TCAD I + II, increased significantly between groups (I = 23%, II = 33%, III = 84%, $p < 0.05$), and involved only single coronary territories in TCAD I but multiple vessels in TCAD II + III. Infarct-atypical CE-MRI was equally distributed across all TCAD stages (I = 50% vs. II = 58% vs. III = 42%, p = NS) without relation to a coronary territory. Patients with only infarct-atypical CE-MRI were associated with significantly better left ventricular function compared with patients with infarct-typical or combined CE-MRI patterns (ejection fraction = 66 ± 6% vs. 45 ± 16% or 60 ± 13%; end-diastolic volume = 139 ± 32 ml vs. 148 ± 27 ml or 164 ± 43 ml; end-systolic volume = 47 ± 15 ml vs. 81 ± 27 ml or 69 ± 38 ml, p ≤ 0.05).

Conclusions CE-MRI allows identification of silent MI in apparently event-free HTX patients and is able to disclose myocardial fibrosis already in patients with absent or mild angiographic TCAD. CE-MRI might be helpful to establish an earlier TCAD diagnosis and to intensify medical treatment. Future studies are necessary to test prognostic implications associated with CE-MRI patterns. (J Am Coll Cardiol 2008;52:1160–7) © 2008 by the American College of Cardiology Foundation

Heart transplantation (HTX) is the ultimate therapy for patients with end-stage heart failure. Worldwide, nearly 4,000 patients receive HTX/year (1). Knowledge of preoperative and post-operative medical treatment and management as well as improvement in surgical techniques has increased tremendously in the last 2 decades, resulting in improved graft survival and patient outcome (1,2).

Nowadays, chronic sequels such as interstitial myocardial fibrosis due to immunosuppressive therapy as well as elevated immune-activated vascular atherosclerosis, also called transplant coronary artery disease (TCAD), play a more advanced role in the aftercare of HTX (3).

See page 1168

TCAD is an allograft pan-arterial disease characterized by diffuse concentric and longitudinal intima hyperplasia affecting the entire graft coronary artery vasculature and is associated with major adverse cardiac events (4). The reference standard for TCAD detection is intravascular ultrasound (IVUS) (5), but due to high cost and the limited availability of IVUS, coronary angiography (fluoroscopy) is usually performed (6). Consequently, subclinical TCAD is frequently overlooked, and patients do not receive adequate therapy. Furthermore, standard angiography lacks informa-

From the Abteilung Innere Medizin III, Medizinische Klinik, Universitätsklinikum Heidelberg, Heidelberg, Germany. The authors had full access to the data and take responsibility for its integrity. All authors have read and agree to the article as written. Drs. Steen and Merten contributed equally to this work.

Manuscript received November 13, 2007; revised manuscript received March 3, 2008, accepted May 21, 2008.

tion about the intramural state of TCAD-associated atherosclerosis (7,8).

Additionally, routine annual medical HTX assessment including invasive coronary fluoroscopy exposes patients to a substantial radiation dose and to the hazard of nephro-toxic contrast agents (9). Another inherent problem of fluoroscopy angiography is the lack of tissue information, making potentially hazardous myocardial biopsies necessary for the estimation of commencing tissue rejection processes or myocardial fibrosis (10).

To circumvent these shortcomings in staging HTX patients, a noninvasive approach with advanced tissue characterization would be a helpful tool (11).

Magnetic resonance imaging (MRI) is a noninvasive and nonradiation imaging technique offering excellent tissue contrast and superior image quality (12).

By administration of gadolinium contrast agents in combination with specific MRI imaging sequences, delayed contrast-enhanced (CE) MRI enables further high-resolution tissue characterization. Intramural, diffuse, or subepicardial infarct-atypical versus acute or chronic infarct-typical subendocardial fibrosis with various degrees of transmurality can be distinctly differentiated (13).

In the present study we sought to apply CE-MRI to investigate its feasibility to assess the prevalence of infarct-typical and -atypical myocardial fibrosis in patients after HTX. We further hypothesized that in patients with fluoroscopy classified mild TCAD we would already detect either chronic infarct-typical or -atypical or a combination of CE-MRI patterns and could therefore further subclassify HTX patients on a tissue level.

Methods

Study population. From October 2004 until December 2005 we studied 53 consecutive asymptomatic adult HTX patients, including 42 men and 11 women. The study was approved by the institutional review committee, and patients gave informed consent.

Coronary angiography. Coronary angiography was performed by the femoral approach with standard fluid-filled catheters within 4 weeks of MRI scans. All patients underwent right and left heart catheterization and endomyocardial biopsy. Angiograms were obtained from multiple projections and interpreted qualitatively by 2 independent observers blinded to the MRI data analysis.

Angiographic classification of TCAD. Angiographic estimation of allograft TCAD in epicardial coronary arteries was semi-quantitatively standardized with the following criteria: I = mild evidence of TCAD, II = manifest TCAD with focal lesions <30% to 75% stenosis, and III = severe TCAD with focal lesions ≥75% or need for interventional treatment.

Rejection score and rejection treatment/year score. Routine endomyocardial biopsies were performed on an annual basis. Cardiologists and cardiology fellows performed all biopsies; experienced cardiac pathologists reviewed and graded the biopsy specimens according to International Society for Heart and Lung Transplantation (ISHLT) criteria (14). A rejection index was calculated as follows: ISHLT rejection grades were assigned a point score (ISHLT 0/1A ¼ = 0 points, 1B ¼ = 1 point, 2 ¼ = 2 points, 3A ¼ = 3 points, 3B ¼ = 4 points, and 4 ¼ = 5 points). The total point score of all biopsy results of a patient was normalized to the number of biopsies performed to yield the rejection index.

MRI protocol. Within 4 weeks of coronary angiography, vector-electrocardiography–triggered CE-MRI was performed on a 1.5-T Whole Body MRI scanner (Philips Medical Systems, Best, the Netherlands) with a cardiac phased-array receiver coil.

Abbreviations and Acronyms

CE-MRI = contrast-enhanced magnetic resonance imaging
EDV = end-diastolic volume
EF = ejection fraction
ESV = end-systolic volume
HTX = heart transplantation
ISHLT = International Society for Heart and Lung Transplantation
IVUS = intravascular ultrasound
LV = left ventricular
MI = myocardial infarction
NT-proBNP = N-terminal part of the pro-B-type natriuretic peptide
TCAD = transplant coronary artery disease
TI = inversion time

Assessment of left ventricular (LV) function and late enhancement (CE-MRI) was performed in a standardized way (15,16) with the following amendments: 10 to 15 min after a dose of 0.2 mmol gadolinium per kilogram of body weight (Magnevist, Schering, Germany), a 3-dimensional sequence with inversion time (TI) scout was used to select the TI, which was typically 180 to 240 ms.

MRI data analysis. An MRI wall motion and contrast enhancement data analysis was carried out on a commercially available cardiovascular magnetic resonance workstation (Philips Viewforum, Version 3.4). Two blinded observers conducted image analysis at least 8 weeks after acquisition. For CE-MRI data analysis, the accredited American Heart Association (AHA) 17-segment model (17) of the LV was employed.

End-diastolic volume (EDV) (milliliters) and end-systolic volume (ESV) (milliliters) with resulting ejection fraction (EF) (%) were generated manually with short-axis volumetry by determination of end-diastolic and -systolic heart phases and subsequent delineation of endocardial borders excluding papillary muscles.

For evaluation of myocardial mass, borders were drawn at the interface between myocardium and epicardium on end-diastolic images including papillary muscles.

CE-MRI. Before analysis, 2 readers classified CE-MRI image quality into diagnostically analyzable or qualitatively unacceptable.

Accordingly, images were divided into infarct-typical bright lesions with subendocardial involvement and variable degrees of transmurality. In contrast, less distinct intramyo-

JACC Vol. 52, No. 14, 2008
September 30, 2008:1160–7

cardial or epimyocardial patchy or nodular enhancing areas omitting the subendocardium were classified as atypical CE-MRI (Fig. 1).

Qualitative infarct size was visually assessed per segment and classified as grade I = <25%, grade II = 26% to 50%, grade III = 51% to 75%, and grade IV = >75% of LV wall thickness.

For quantitative infarct size analysis, we employed a specific scar measurement tool (Philips Viewforum), where infarct size was visually defined as area of CE-MRI on short-axis views. Infarct size was determined visually and drawn manually by delineation of hyperenhanced versus normally saturated dark myocardium. Volume integration of hyperenhanced areas on short-axis slices were considered as absolute infarct masses.

Mean mass of CE-MRI for TCAD I to III was normalized to mean myocardial mass/TCAD group and is given in percent infarcted mass/normal myocardium.

To prove the existence of atypical enhancement we also repeated basal, mid-ventricular, and apical inversion recovery 2-dimensional short-axes (inversion recovery prepared turbo field echo, pixel size = 1.8 × 1.4 mm, slice thickness = 8 mm) MRI with higher resolution with 2 phase-encoding directions to exclude artefact (16) after adjustment of the correct TI time (180 to 240 ms) (18).

Regional CE-MRI distribution and functional assessment of infarct-typical and -atypical enhancement patterns. Myocardial areas of infarct-typical and -atypical CE-MRI were allocated to the AHA 17-segment model (18) to further investigate potential differences in regional distribution patterns.

Statistics. All continuous variables were expressed as mean ± SD. Medians are given with the 25%/75% confidence intervals. Comparison of groups was conducted with analysis of variance statistics. For nonparametric variables we used either the Kruskal-Wallis or the chi-square test for dichotomic variables. A p value ≤0.05 was considered statistically significant.

Results

Study population. We divided our patients into 3 groups (TCAD I to III) following the angiographic criteria. Patient characteristics are shown in Table 1.

Patient age (years), gender, and body mass index (kg/m^2) were not notably different. Patients with TCAD III were transplanted significantly longer ago than TCAD I + II patients ($p < 0.001$). Ischemia time of the transplanted hearts was significantly different among all 3 groups ($p < 0.001$). Interestingly, TCAD III patients had the shortest ischemia time. The rejection score and

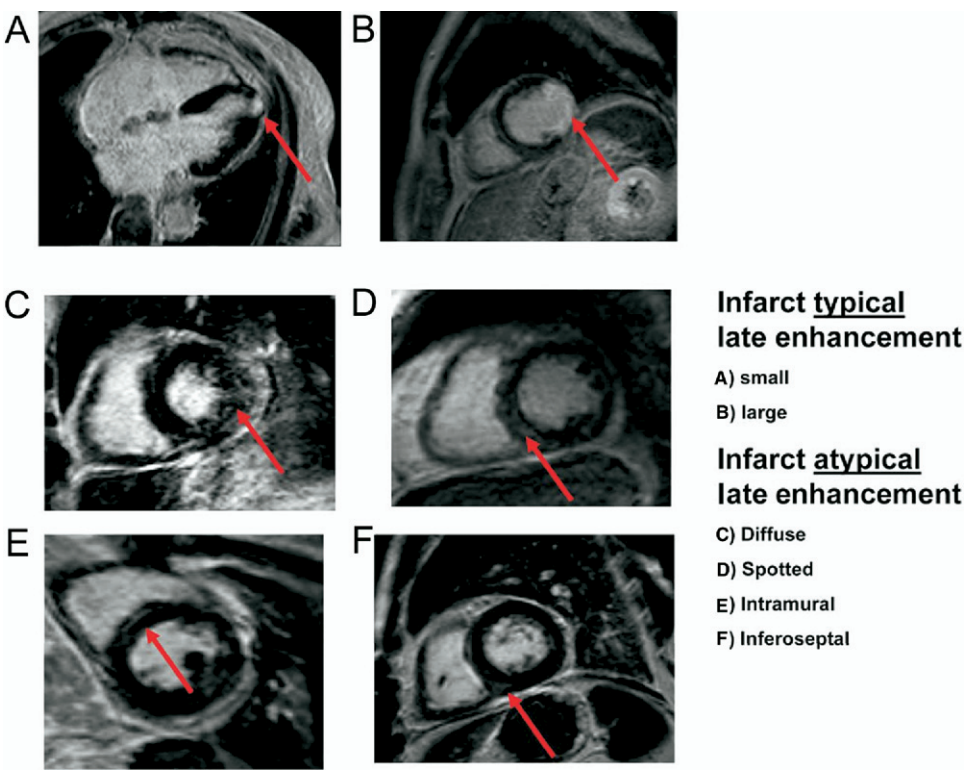

Figure 1 Distribution and Percentage of Murality of Myocardial Infarctions in Transplant Coronary Artery Disease I to III

Infarct-typical **(A, B)** and -atypical **(C to F)** contrast-enhanced magnetic resonance imaging patterns. The **red arrows** point to the contrast-enhanced lesions.

Table 1 Patient Characteristics

	TCAD I	TCAD II	TCAD III	p Value
Heart recipient				
Number of patients	28	15	10	
Gender (% female)	6 (21%)	2 (13%)	3 (30%)	
BMI (kg/m^2)	25.7 ± 4.8	27.2 ± 3.4	25.0 ± 4.3	NS
Age (yrs)	57 ± 11.6	53.9 ± 12.7	61.0 ± 10.8	NS
Years after HTX	5.8 ± 4.5	6.5 ± 3.8	11.9 ± 4.5	<0.001
Rejection score	0.3 ± 0.3	0.3 ± 0.3	0.3 ± 0.2	NS
Ischemia time of TX heart (min)	170 ± 52	194 ± 46	157 ± 34	<0.001
Heart recipient cardiovascular risk factors				
Hypertension	16 (57%)	13 (87%)	5 (50%)	NS
Diabetes	6 (25%)	2 (13%)	5 (50%)	NS
LDL (mg/dl)	102.7 ± 22.4	95.2 ± 19.5	95.2 ± 18.7	NS
HDL (mg/dl)	57.1 ± 11.3	51.0 ± 9.8	51.0 ± 8.3	NS
Cytomegalie virus infection	9 (32%)	4 (27%)	1 (10%)	NS
Heart recipient basic heart parameters				
Heart rate	81.2 ± 11.1	82.0 ± 12.3	74.0 ± 14.1	NS
EF (%)	63.7 ± 9.8	63.6 ± 10.2	48.8 ± 13.3	<0.01
EDV (ml)	139.0 ± 26.1	152.7 ± 23.2	167.6 ± 44.9	NS
ESV (ml)	50.2 ± 18.2	55.6 ± 18.1	85.1 ± 44.9	<0.01
CO (l/min)	7.1 ± 1.7	7.8 ± 1.4	5.8 ± 1.4	<0.01
SV (ml)	83.8 ± 24.0	97.1 ± 21.5	78.5 ± 24.6	NS
Mass (g)	100.5 ± 27.6	102.7 ± 24.5	110.4 ± 27.8	NS
Heart recipient serum parameters				
cTnT pts with elevated levels	3 (10%)	1 (7%)	4 (40%)	
cTnT (ng/dl)	0.01 ± 0.03	0.01 ± 0.05	0.02 ± 0.03	NS
NT-proBNP pts with >125 ng/l levels (%)	24 (86%)	13 (87%)	10 (100%)	
Median NT-proBNP (mg/dl) (25%–75% percentiles)	537 (160–1,106)	643 (235–1,009)	2,505 (680–4,273)	<0.001
Creatinine pts with elevated levels >1.5 mg/dl (%)	27 (96%)	12 (80%)	9 (90%)	
Creatinine (mg/dl)	1.4 ± 0.6	1.5 ± 0.9	1.7 ± 0.6	NS
Concomitant diseases				
ESRD	22	8	5	NS
Peripheral artery disease	3	0	0	NS
COPD	3	2	2	NS
Monoclonal immunoglobulinopathy	2	0	3	NS
Osteoporosis/osteopenia	2	2	0	NS
Heart donor				
Donor age	35.0 ± 12.2	36.9 ± 11.9	41.4 ± 14.9	NS
Donor gender (% female)	15 (54%)	5 (33%)	7 (70%)	
Indications for heart transplantation				
DCM	16	11	6	
Ischemic cardiomyopathy	9	3	3	
Valvular cardiomyopathy	1	1	0	
Constrictive pericarditis	1	0	0	
Myocarditis	1	0	1	

BMI = body mass index; CO = cardiac output; COPD = chronic obstructive pulmonary disease; cTnT = cardiac troponin T; DCM = dilated cardiomyopathy; EDV = end-diastolic volume; EF = ejection fraction; ESRD = end stage renal disease; ESV = end-systolic volume; HDL = high-density lipoprotein; HTX = heart transplantation; LDL = low-density lipoprotein; NT-proBNP = N-terminal part of the pro-B-type natriuretic peptide; pts = patients; TCAD I = no evidence of TCAD; TCAD II = established TCAD with lesions <75% stenosis; TCAD III = severe TCAD with lesions ≥75% or need for interventional treatment.

rejection treatment/year score as well as heart recipient cardiovascular risk factors were also not significantly dissimilar.

When compared with TCAD I + II patients, recipients with TCAD III had significantly lower EF (49 ± 13% vs. 64 ± 10% vs. 64 ± 10%, $p < 0.01$), higher ESV (85 ± 34 ml vs. 50 ± 18 ml vs. 56 ± 18 ml, $p < 0.01$), and lower cardiac output (5.8 ± 1.4 ml vs. 7.1 ± 1.7 ml vs. 7.8 ± 1.4 ml, $p < 0.01$), whereas baseline heart rate, EDV, stroke volume, and myocardial mass were not significantly different.

The N-terminal part of the pro-B-type natriuretic peptide (NT-proBNP) levels in all 3 groups were significantly elevated (cut-off value >125 ng/l) and differed significantly. Moreover, between 80% and 93% of the patients showed a chronic renal impairment (creatinine levels >1.5 mg/dl) with no significantly different creatinine levels between TCAD I to III patients.

JACC Vol. 52, No. 14, 2008
September 30, 2008:1160–7

MRI results. After consensus reading of 2 experienced analysts, CE-MRI image quality was acceptable in 22 of 28 TCAD I (79%), 12 of 15 TCAD II (80%), and 7 of 10 TCAD III (70%) patients. The reasons for the 12 unacceptable CE-MRI scans were as follows: 1) nonspecified arrhythmia (5); 2) inadequate electrocardiography-triggering (6); 3) commencing hyperventilation; and/or 4) claustrophobia during the study.

CE-MRI patterns. Figure 1 indicates the different patterns of CE-MRI in HTX patients. Figures 1A and 1B present an infarct-typical small focal and large transmural myocardial infarction (MI).

Morphologically, 4 different forms of infarct-atypical gadolinium accumulations could be distinguished: diffuse lesions with patchy and transmural CE-MRI (Fig. 1C); spotted, more sharply distinguishable intramural bright lesions (Fig. 1D); less distinguishable intramural lesions (Fig. 1E); or infero-septal sharply circumscribed lesions of delayed CE-MRI (Fig. 1F).

Mean infarct-typical myocardial mass was 3.2% for TCAD I, 4.1% for TCAD II, and 9.9% for TCAD III ($p < 0.05$).

Distribution and percentage of CE-MRI in TCAD I to III. As shown in Figure 2A, 5 TCAD I (23%), 4 TCAD II (33%), and 6 TCAD III (84%) patients had infarct-typical CE-MRI lesions. Interestingly, even in patients with TCAD I having inconspicuous angiographies, nearly every fourth patient revealed typical MI CE-MRI patterns.

Transmural infarcts were present in TCAD I to III, whereas 51% to 75% CE-MRI could be seen in TCAD I + III and 26% to 50% CE-MRI lesions were observed in TCAD II + III. Less than 25% transmural extent of CE-MRI was not present in any of the groups.

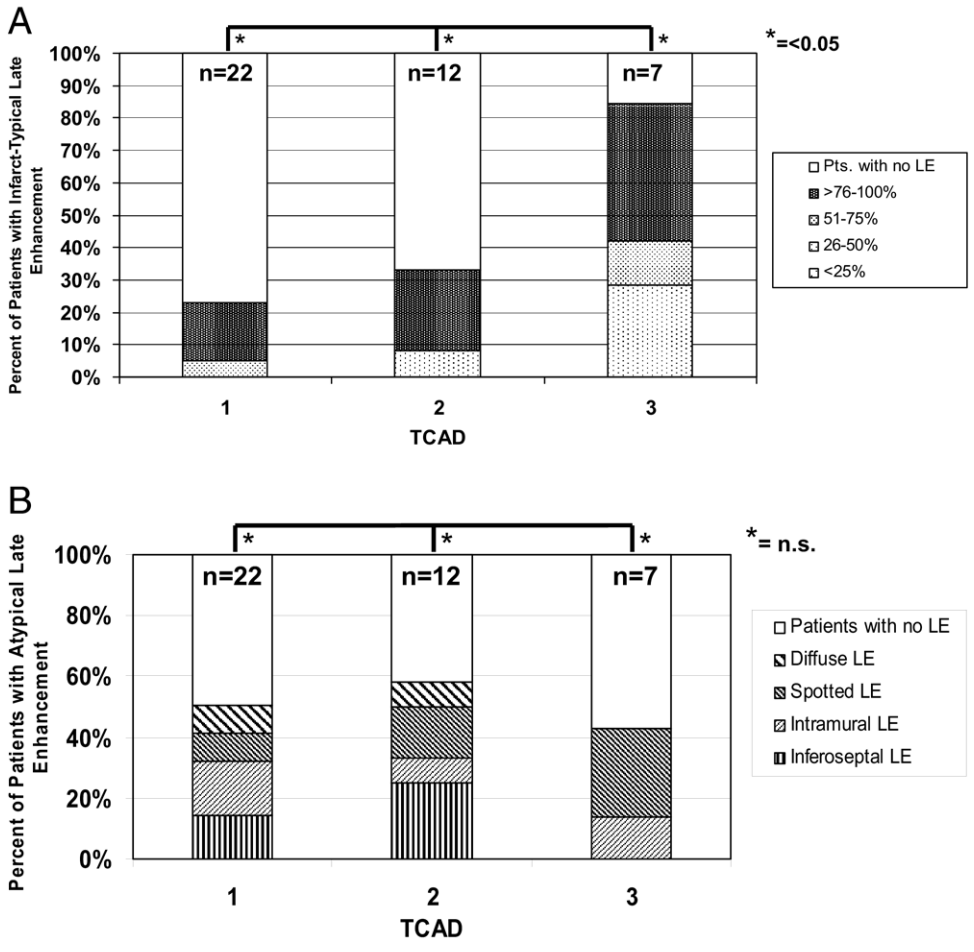

Figure 2 Distribution and Percentage of Typical and Atypical Late Enhancement in TCAD I to III

(A) Comparison of the percentage of patients with infarct-typical contrast-enhanced magnetic resonance imaging (CE-MRI) and their distribution and murality of myocardial infarction in all 3 transplant coronary artery disease (TCAD) groups. Note the significant increase of infarct-typical lesions from TCAD I to III. The transmurality index was at least 25% to 50%. **(B)** Comparison of the percentage of patients with infarct-atypical CE-MRI and their distribution in all 3 TCAD groups. For infarct-atypical CE-MRI the presence of CE-MRI was evenly distributed among the groups. LE = late enhancement.

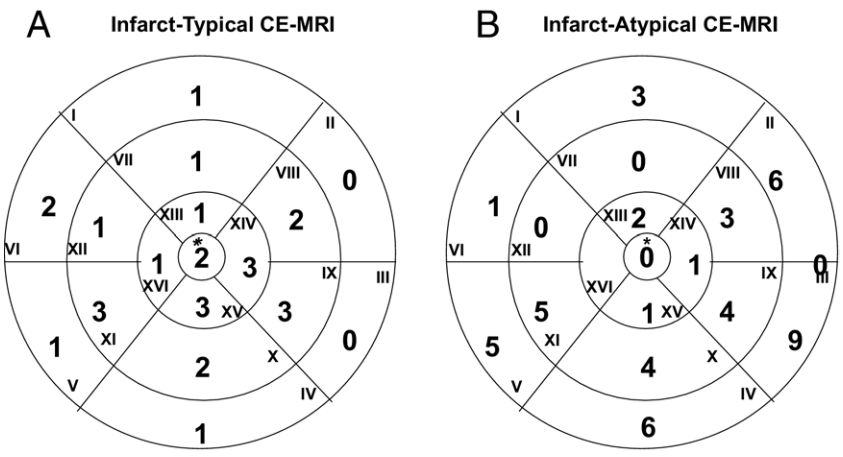

Figure 3 **Distribution Patterns of Infarct-Typical and -Atypical CE-MRI**

Distribution of all affected infarct-typical **(A)** and -atypical **(B)** contrast-enhanced magnetic resonance imaging (CE-MRI) segments related to the American Heart Association 17-segment model. Of infarct-typical lesions, 81% were accentuated in the mid-ventricular (segments VII to XII) and apical (XIII to XVII) segments. In contrast, 60% of infarct-atypical areas were accentuated at basal slices, predominantly lateral and inferior. *Segment XVII.

Generally, an increasing number of patients with infarct-typical CE-MRI patterns could be observed with increasing severity of TCAD.

Spotted and intramural CE-MRI was evenly present in TCAD I to III (50% vs. 58% vs. 42%, p = NS), whereas inferoseptal and diffuse patterns could be observed only in TCAD I + II (Fig. 2B).

Distribution of infarct-typical/-atypical CE-MRI in the AHA 17-segment model. Figure 3 displays the distribution of all affected infarct-typical and -atypical CE-MRI segments related to the AHA 17-segment model. In general, of 27 affected infarct-typical segments, 22 (81%) were accentuated in the mid-ventricular (segments VII to XII) and apical (XIII to XVII) segments. Only 5 infarcts (19%) were observed at basal slices.

In contrast, of 50 affected infarct-atypical segments, the overall majority of 30 segments (60%) were accentuated at basal slices (segments I to VI) and only 20 atypical CE-MRI patterns (40%) were observed in mid-ventricular and apical slices (VII to XVII).

Myocardial function and mass in infarct-typical, infarct-atypical, and combined CE-MRI. To further investigate the effects of MI on cardiac function and mass, HTX patients have been categorized into: 1) infarct-typical; 2) infarct-atypical; and 3) combined infarct-typical and -atypical CE-MRI independent of their prior angiographically assessed degree of TCAD (Table 2).

Compared with patients with atypical or combined CE-MRI, patients with typical infarcts showed significantly lower ejection fractions (45 ± 16% vs. 66 ± 6% and 60 ± 13%) and significantly higher EDV (148 ± 27 ml vs. 139 ± 32 ml vs. 164 ± 43 ml, p = 0.05) and ESV (81 ± 27 ml vs. 47 ± 15 ml and 69 ± 38 ml). Differences in stroke volume and myocardial mass failed to reach statistical significance. Comparing combined with only infarct-atypical CE-MRI patients, the difference for EF and ESV also proved to be statistically significant (both $p < 0.05$).

Discussion

Tissue characterization with CE-MRI allows an earlier identification of TCAD, even in the absence of angiographic changes. Accordingly, we detected infarct-typical CE-MRI areas suggesting silent MI in an apparently event-free HTX cohort.

Table 2 **Myocardial Function and Mass in Infarct-Typical, Infarct-Atypical, and Combined CE-MRI**

	Infarct-Typical CE-MRI (n = 6)	Infarct-Atypical CE-MRI (n = 12)	Combined CE-MRI (n = 9)	p Value	Significance
EF (%) ± SD	45 ± 16	66 ± 6	60 ± 13	0.035	Yes
EDV (ml) ± SD	148 ± 27	139 ± 32	164 ± 43	0.05	Yes
ESV (ml) ± SD	81 ± 27	47 ± 15	69 ± 38	0.045	Yes
SV (ml) ± SD	64 ± 28	92 ± 21	85 ± 34	0.145	No
Myocardial mass (g) ± SD	100 ± 17	98 ± 21	117 ± 34	0.24	No

CE-MRI = contrast-enhanced magnetic resonance imaging; EDV = end-diastolic volume; EF = ejection fraction; ESV = end-systolic volume; SV = stroke volume.

Prevalence and distribution of infarct-typical CE-MRI. We found that infarct-typical CE-MRI was already present in about one-fourth of TCAD I and one-third of TCAD II patients with significant differences ($p < 0.05$) between the groups.

Because the transplanted hearts were echocardiographically classified as free of previous MI, it is tempting to speculate that these patients had suffered silent subclinical MI after HTX and might have been missed by routine coronary angiography because corresponding angiograms in TCAD I showed no or only mild narrowing of epicardial arteries.

In the earlier stages of TCAD, the narrowing of the intima is more likely to cause microinfarctions, whereas a more advanced coronary affection might also result in larger infarcts. Consistently, we found single small infarct-typical CE-MRI patterns in TCAD I and multiple late enhancement lesions of variable size in TCAD II and III.

Infarct-typical segments were more often found in mid-ventricular and apical segments. This observation is consistent with the angiographic appearance of TCAD showing predominantly subsegmental rarefication of coronary arteries (19). Due to the diffuse concentric affection of the entire coronary artery, smaller vessels are more prone to occlusion than larger branches (19,20).

As proposed by Glagov et al. (7), in common atherosclerosis luminography does not represent the intramural state of the inflammatory atherosclerotic process, because positive coronary arterial remodeling or vessel wall thickening are only detected by IVUS (20). Therefore, non-invasive tissue characterization by CE-MRI would greatly enhance our knowledge of the vascular TCAD affection in HTX patients.

Our observations highlight the importance of MRI as a complementary tool in the follow-up of HTX. Because MI in HTX patients is associated with major adverse cardiac events and poor prognosis (1,2), 22% of TCAD I patients with already subsided MI would have been overlooked or misclassified by fluoroscopy angiography. However, further clinical studies are needed to show the correlation between the existence or severity of CE-MRI lesions and adverse clinical outcomes.

The presence of infarct-typical CE-MRI was associated with a significantly worse LV function and higher EDV and ESV. Also, levels for NT-proBNP among all 3 TCAD groups were significantly elevated, although creatinine levels were not dissimilar between groups.

Because LV function and volume as well as elevated NT-proBNP levels have a future prognostic relevance in nontransplanted cardiac patients, one might hypothesize about the role of NT-proBNP in this patient collective. Given that NT-proBNP levels correlate with the TCAD stage, it is reasonable to presume that NT-proBNP levels could serve as an independent predictor of advanced TCAD (data on file, not shown) and could also be useful to rule out advanced TCAD stages.

Prevalence and distribution of infarct-atypical CE-MRI. Infarct-atypical CE-MRI was found in approximately 50% of all cases, suggesting that fibrosis was evenly distributed across all TCAD stages.

By its visual appearance, infarct-atypical CE-MRI could be described as diffuse, spotted, intramural, or localized (antero-/inferoseptal) without colocalization to specific coronary territories.

In our patient cohort, no correlation was found between atypical CE-MRI and the different TCAD stages. The exact patho-mechanism for the occurrence of infarct-atypical CE-MRI patterns is yet unclear. Potential reasons include presence of end-stage renal disease (21), the amount of organ rejections or pharmacological interventions against organ rejections, cytomegalovirus or other opportunistic infections, former myocarditis (22), or other immune processes (23). In our study we could not conclusively demonstrate whether the missing correlation between atypical late enhancement and organ rejections or immunosuppressive interventions was only due to small sample size or whether any of the numerated factors played a significant role in the generation of myocardial enhancement patterns. Again, further studies with larger patient numbers are needed to evaluate this lack of correlation more in depth, potentially employing targeted biopsies in combination with immunohistological techniques.

Infarct-atypical distribution patterns were predominantly detected in basal and mid-ventricular areas. Predominantly these areas are prone to infarct-atypical CE-MRI patterns with histologically proven storage of pathologic proteins, as is known from storage diseases such as amyloidosis (24), Anderson-Fabry disease (25), or other glycogen storage diseases (26). Whether a comparable patho-mechanism could also be responsible for similar CE-MRI patterns in HTX patients is yet unknown and warrants further investigation.

In our study we employed 0.2 mmol/kg bodyweight gadolinium for the myocardial tissue characterization. Because chronic renal disease was prevalent in most patients and since only recently there is convincing evidence that gadolinium contrast agents could be linked to nephrogenic systemic fibrosis (27), restrictive contrast agent administration would be mandatory. Also, potentially nephrotoxic medication should be discontinued before MRI, the patient should be well hydrated, creatinine levels should be followed up, or even hemodialysis after MRI should be considered (28,29).

Study limitations. This pilot study described CE-MRI abnormalities in a well-defined HTX population and was neither intended nor powered to evaluate the prognostic role of magnetic resonance abnormalities.

The stage of TCAD might have been underestimated by the use of coronary angiography instead of IVUS. However, coronary angiography is more commonly used in clinical

practice and represents the reference method for classification for TCAD.

No correlation was found between atypical CE-MRI and organ rejections, immunosuppressive therapies, infections, myocarditis, or renal impairment (23). Further studies with a larger sample size and targeted myocardial biopsies are needed to investigate potential underlying pathological mechanisms.

The high rate of suboptimal imaging quality (approximately 20%) in contrast to previously published data reflected our intention to reduce selection bias by inclusion of consecutive patients. We did not exclude patients with rhythm and conductance disorders. As a consequence, our results might underestimate the true prevalence of atypical and to a lesser degree typical enhancement due to poorer or noninterpretable image quality.

Conclusions

CE-MRI allowed identification of silent MI in an apparently event-free HTX population and was able to disclose myocardial fibrosis already in patients with absent or mild angiographic TCAD. Because subtle MI and beginning microvascular dysfunction might be missed with conventional coronary angiography, CE-MRI could be helpful to establish an earlier diagnosis and to intensify medical treatment. Future studies are necessary, however, to test prognostic implications associated with CE-MRI patterns.

Acknowledgments

The authors specifically want to acknowledge the work of our magnetic resonance technicians, B. Hoerig, Jeanette Köppert, and Angela Stöcker-Wochele, who conducted the MRI scans.

Reprint requests and correspondence: Dr. Evangelos Giannitsis, Abteilung Innere Medizin III, Medizinische Klinik, Universitätsklinikum Heidelberg, 69120 Heidelberg, Germany. E-mail: evangelos_giannitsis@med.uni-heidelberg.de.

REFERENCES

1. Bennett LE, Keck BM, Daily OP, Novick RJ, Hosenpud JD. Worldwide thoracic organ transplantation: a report from the UNOS/ISHLT International Registry for Thoracic Organ Transplantation. Clin Transpl 2000;31–44.
2. Robbins RC, Barlow CW, Oyer PE, et al. Thirty years of cardiac transplantation at Stanford university. J Thorac Cardiovasc Surg 1999;117:939–51.
3. Kocik M, Malek I, Janek B, Zelizko M, Pirk J. Risk factors for the development of coronary artery disease of a grafted heart as detected very early after orthotopic heart transplantation. Transpl Int 2007;20:666–74.
4. Li H, Tanaka K, Anzai H, et al. Influence of pre-existing donor atherosclerosis on the development of cardiac allograft vasculopathy and outcomes in heart transplant recipients. J Am Coll Cardiol 2006;47:2470–6.
5. Nicolas RT, Kort HW, Balzer DT, et al. Surveillance for transplant coronary artery disease in infant, child and adolescent heart transplant recipients: an intravascular ultrasound study. J Heart Lung Transplant 2006;25:921–7.
6. Weis M, von Scheidt W. Coronary artery disease in the transplanted heart. Annu Rev Med 2000;51:81–100.
7. Glagov S, Weisenberg E, Zarins CK, Stankunavicius R, Kolettis GJ. Compensatory enlargement of human atherosclerotic coronary arteries. N Engl J Med 1987;316:1371–5.
8. Li HY, Tanaka K, Oeser B, Wertman B, Kobashigawa JA, Tobis JM. Compensatory enlargement in transplant coronary artery disease: an intravascular ultrasound study. Chin Med J (Engl) 2006;119:564–9.
9. Erley CM, Bader BD. [Consequences of intravascular contrast media on kidney function—risk and prevention]. Rofo 2000;172:791–7.
10. Billingham ME, Cary NR, Hammond ME, et al. A working formulation for the standardization of nomenclature in the diagnosis of heart and lung rejection: Heart Rejection Study Group. The International Society for Heart Transplantation. J Heart Transplant 1990;587–93.
11. Vriens PW, Blankenberg FG, Stoot JH, et al. The use of technetium Tc 99m annexin V for in vivo imaging of apoptosis during cardiac allograft rejection. J Thorac Cardiovasc Surg 1998;116:844–53.
12. Jackson E, Bellenger N, Seddon M, Harden S, Peebles C. Ischaemic and non-ischaemic cardiomyopathies—cardiac MRI appearances with delayed enhancement. Clin Radiol 2007;62:395–403.
13. Mahrholdt H, Wagner A, Judd RM, Sechtem U, Kim RJ. Delayed enhancement cardiovascular magnetic resonance assessment of non-ischaemic cardiomyopathies. Eur Heart J 2005;26:1461–74.
14. Billingham ME, Cary NR, Hammond ME, et al. A working formulation for the standardization of nomenclature in the diagnosis of heart and lung rejection: heart rejection study group. The International Society for Heart Transplantation. J Heart Transplant 1990;9:587–93.
15. CMR Image Acquisition Protocols. Available at: http://www.scmr.org/documents/scmr_protocols_2007.pdf. Accessed April 11, 2007.
16. Steen H, Giannitsis E, Futterer S, Merten C, Juenger C, Katus HA. Cardiac troponin T at 96 hours after acute MI correlates with infarct size and cardiac function. J Am Coll Cardiol 2006;48:2192–4.
17. Cerqueira MD, Weissman NJ, Dilsizian V, et al., American Heart Association Writing Group on Myocardial Segmentation and Registration for Cardiac Imaging. Standardized myocardial segmentation and nomenclature for tomographic imaging of the heart: a statement for healthcare professionals from the Cardiac Imaging Committee of the Council on Clinical Cardiology of the American Heart Association. Circulation 2002;105:539–42.
18. Assomull RG, Prasad SK, Lyne J, et al. Cardiovascular magnetic resonance, fibrosis, and prognosis in dilated cardiomyopathy J Am Coll Cardiol 2006;48:1977–85.
19. Gao SZ, Alderman EL, Schroeder JS, Silverman JF, Hunt SA. Accelerated coronary vascular disease in the heart transplant patient: coronary arteriographic findings. J Am Coll Cardiol 1988;12:334–40.
20. Billingham ME. Graft coronary disease: the lesions and the patients. Transplant Proc 1989;21:3665–6.
21. Mark PB, Johnston N, Groenning BA, et al. Redefinition of uremic cardiomyopathy by contrast-enhanced cardiac magnetic resonance imaging. Kidney Int 2006;69:1839–45.
22. Mahrholdt H, Wagner A, Deluigi CC, et al. Presentation, patterns of myocardial damage, and clinical course of viral myocarditis. Circulation 2006;114:1581–90.
23. Pereira NL, Zile MR, Harley RA, Van Bakel AB. Myocardial mechanisms causing heart failure early after cardiac transplantation. Transplant Proc 2006;38:2999–3003.
24. Maceira AM, Joshi J, Prasad SK, et al. Cardiovascular magnetic resonance in cardiac amyloidosis. Circulation 2005;111:186–93.
25. Moon JC, Sheppard M, Reed E, Lee P, Elliott PM, Pennell DJ. The histological basis of late gadolinium enhancement cardiovascular magnetic resonance in a patient with Anderson-Fabry disease. J Cardiovasc Magn Reson 2006;8:479–82.
26. Moon JC, Mundy HR, Lee PJ, Mohiaddin RH, Pennell DJ. Images in cardiovascular medicine. Myocardial fibrosis in glycogen storage disease type III. Circulation 2003;107:e47.
27. Marckmann P, Skov L, Rossen K, et al. Nephrogenic systemic fibrosis: suspected causative role of gadodiamide used for contrast-enhanced magnetic resonance imaging. J Am Soc Nephrol 2006;17:2359–62.
28. Rodby RA. Dialytic therapies to prevent NSF following gadolinium exposure in high-risk patients. Semin Dial 2008;21:145–9.
29. Thomsen HS, Morcos SK (2003) Contrast media and the kidney: European Society of Urogenital Radiology (ESUR) guidelines. Br J Radiol 76:513–8.

Key Words: atherosclerosis ■ coronary artery disease ■ heart transplantation ■ magnetic resonance imaging ■ myocardial infarction.